Basic Coandă MAV Fluid Dynamics and Flight Mechanics

H Djojodihardjo[1]and RI Ahmed[2]
[1]The Institute for the Advancement of Aerospace Science and Technology, Jakarta, Indonesia;
[2]Graduate Student, Aerospace Engineering Department, Universiti Putra Malaysia;
[1]harijono.djojodihardjo@yahoo.com; [2]engriyadh64@gmail.com

Abstract. Capitalizing on the basic fundamental principles, the Fluid Dynamics and Flight Mechanics of a semi-spherical Coandă MAV configurations are revisited and analyzed as a baseline. A mathematical model for a spherical Coandă MAV in hover and translatory motion is developed and analyzed from first physical principles. To gain further insight into the prevailing flow field around a Coandă MAV, as well as to verify the theoretical prediction presented in the work, a computational fluid dynamic CFD simulations for a Coandă MAV generic model are elaborated. The mathematical model and derived performance measures are shown to be capable in describing the physical phenomena of the flow field of the semi-spherical Coandă MAV. The relationships between the relevant parameters of the mathematical model of the Coandă MAV to the forces acting on it are elaborated subsequently.

Keywords: Circulation control, Coandă effect, Coandă MAV Flight Dynamics, Coandă MAV Fluid Dynamics, Micro air vehicle (MAV), Unmanned Air Vehicle (UAV)

1. Introduction

Coandă effect and Coandă jet have been found and utilized for flow control in many applications in engineering and health science, among others, such as in aircraft and vehicle technology [1-5], wind-turbines [6-9], and upper respiratory system [10]. The science of flow control can be traced back to Prandtl in his seminal paper in 1904 with his breakthrough in the science of fluid mechanics by introducing the boundary-layer theory and elucidated the physics of the separation phenomena and the control of the boundary layers. Various Coandă MAV configurations have been proposed and developed. In the design and operation of a Coandă MAV which could meet the desired mission and design requirements, the basic working relationships among various relevant variables and parameters governing the aerodynamics forces should be established. To assist the analysis, design and developments of Coandă MAV's, several tools can be resorted to. The first is the analytical tool, which capitalizes on the basic fundamental principles. The second is the utilization of Computational Fluid Dynamics (CFD) which has the advantage of providing visualization for significant insight and identification to the problem. In addition, CFD visualization can be utilized in gaining better insight and identifying specific details. Experimental tools can benefit from the insight gained by analysis, CFD computational and visualization studies, in the preliminary study stage by designing specific experiments as well as in the conceptual and prototype design stages. The analysis carried out here is associated with hovering and cruising conditions, which should give further insight on and can be further elaborated into Coandă MAV maneuvering performance.

The present analysis is carried out on Coandă MAV spherical configuration as a baseline, which utilizes some results from the authors' previous analysis. The equations can be easily modified for other configurations and can be compared to other investigators' results for further assessments. CFD visualization studies will also be utilized to gain further understanding in developing the physical model in the analysis.

In the model development and analysis of a semi-spherical Coandă MAV, a propulsion system is utilized to introduce a Coandă jet blanket which is deflected downward due to the curved upper surface of

the vehicle, to provide both hover as well as cruise capabilities. Thus lift will be generated, first to hover and later for cruise propulsion. Such Coandă jet has been utilized for circulation enhancement for fixed wing aircraft in forward flight and turbine blades movement [3-9]. The principle of Coandă MAV lift generation as well as the equation of motion for its translatory motion will be derived and elaborated.

Some basic results drawn from the physical and mathematical model has been obtained to describe the physical phenomena of the flow field related to the relevant surfaces influenced by the Coandă effect jet sheets, and rewritten in a more convenient form as necessary to gain better insight on the relationship among the relevant parameters.

2. Fluid Dynamic Analysis for hovering Semi-spherical Coandă MAV as a Baseline Configuration

The mathematical model of Coandă MAV elaborated here follows closely that of Ahmed et al [10-11] and Djojodihardjo and Ahmed [12-13], which was based on first principles and are summarized and reproduced here as a baseline reference for successive development. For Coandă MAV with the configuration depicted in Figure 1, an actuator rotor can be visualized to be located at the center of the body. For conceptual development, the dimension of the rotor can be set to be small as necessary. Part of the flow being drawn by the actuator can be utilized for lift (like in a helicopter), and part of it will be utilized for introducing radial flow on the surface of the body as a Coandă jet blanket. Momentum analysis is carried out in the analysis of Coandă effect related to finding the relevant aerodynamic forces and defining the Coandă MAV performance parameters. The latter is developed for a baseline and simplified semi-spherical Coandă MAV as depicted in Figure 3(b).

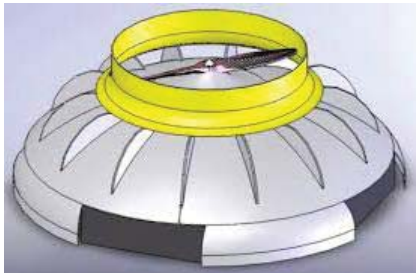

Figure 1: An impression of semi-spherical Coandă MAV configuration utilizing a propeller to develop Coandă jet over its upper surface

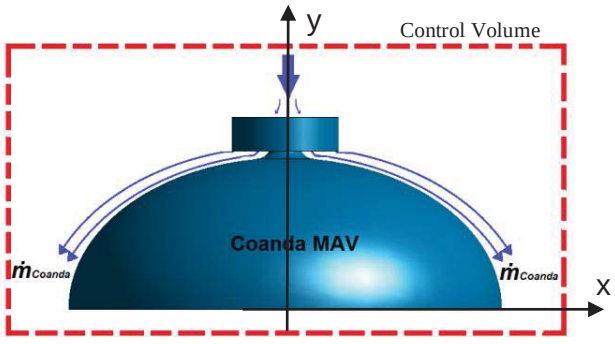

Figure 2: An equivalent semi-spherical Coandă MAV for generic analysis.

In the following, a rigorous analysis is carried out to elaborate how Coandă effect contributes to the generation of lift capability of Coandă MAV. First, the analysis will address the Coandă effect for lift by applying the fundamental conservation analysis on the control volume CV (red dashed rectangle in Figure 2).

Applying the continuity equation on the control volume, which reduces to the Coandă Blanket as depicted in Figure 3, there is obtained

$$\rho \cdot V_{j\text{-}R} \cdot 2\pi Rh = \rho \cdot V_{j\text{-}in} \cdot 2\pi R_i h_i = \rho \cdot V_{j\text{-}out} \cdot 2\pi R_o h_o \tag{1}$$

and

$$V_{j\text{-}R} = \frac{R_i h_i}{Rh_R} V_{j\text{-}in} = \frac{\dot{m}}{2\pi\rho Rh_R} \tag{2}$$

$$V_{j\text{-}out} = \frac{R_i h_i}{R_o h_o} V_{j\text{-}in} = \frac{\dot{m}}{2\pi\rho R_o h_o}$$

where $V_{j\text{-}R}$ is the jet flow velocity, R is the vehicle body radius, h is the jet slot thickness and $\dot{m}$ is the jet mass flow rate. The momentum equation applied to the control volume in the y (vertical) direction can be differentiated into the contribution due to the Coandă Blanket momentum and the pressure difference on the body due to Coandă Blanket:

$$\begin{pmatrix} \textit{Total Lift force} \\ \textit{due to Coandă Blanket} \end{pmatrix} = \begin{pmatrix} \textit{Vertical component of momentum} \\ \textit{balance due to Coandă Blanket} \end{pmatrix} + \begin{pmatrix} \textit{Pressure difference on the body} \\ \textit{of MAVsubject to Coandă Blanket} \end{pmatrix} \tag{3}$$

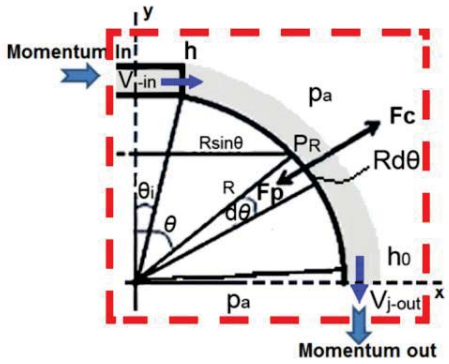

Figure 3: Schematic of Coandă jet blanket for a Spherical MAV momentum balance.

The contribution of lift from the momentum flux through the control volume CV in the y (vertical) direction is given by:

$$\begin{pmatrix} \textit{Force in the} \\ \textit{y-direction} \end{pmatrix} = \begin{pmatrix} \textit{Momentum Out} \\ \textit{in the y-direction} \end{pmatrix} - \begin{pmatrix} \textit{Momentum In} \\ \textit{in the y-direction} \end{pmatrix} \tag{4}$$

Since the Momentum in the radial direction does not contribute to lift, then the momentum equation in the y-direction for the control volume CV depicted in Figure 4 is:

$$F_{\textit{Coanda jet Blanket}} = \dot{m} V_{j\text{-}out} = 2\pi R_i h_i \, \rho \cdot V_{j\text{-}in} \cdot V_{j\text{-}out} \tag{5}$$

The contribution of lift from the pressure difference between the upper part (curved MAV body covered by Coandă jet Blanket) and the lower part of the MAV body can be found by considering various fundamental physical approach. The detail of the elaboration can be found in Ahmed and Djojodihardjo [10-11] and yields**:**

$$F_{Induced\ pressure\ difference} = F_{lower-surface} - F_{upper-surface}$$
$$= \pi\left(R_0^2 - R_i^{\,2}\right) p_a - \int_{\theta_i}^{\theta_0} \left(p_a - \frac{h}{R}\rho\left(\frac{\dot{m}}{2\pi\rho Rh}\right)_{j-R}^{2} \right) \pi R^2 \sin 2\theta d\theta \tag{6}$$

where θ_i and θ_0 are the turning angles at which the jet flow injected and separated from the Coandă surface respectively, as depicted in Figure 3. The jet flow assumed to be uniform outflow separating at the sharp edge of the Coandă MAV curved surface. Then the contribution for lift due to the pressure difference across the surfaces of the MAV body, for the latter approach is given by (as elaborated by Djojodihardjo and Ahmed [12-13]), for the significant value of θ_i):

$$F_{Induced\ pressure\ difference} = \left(\frac{\dot{m}^2}{4\pi\rho h_R R}\right)_{j-R} \tag{7}$$

Hence the total lift due to Coandă jet blanket momentum and Coandă jet blanket induced pressure difference is given by

$$Lift_{\substack{Spherical-Coanda\ jet\ Blanket+ \\ induced\ pressure\ difference}} = 2\pi R_i h_i\ \rho V_{j\text{-}in} \cdot V_{j\text{-}out} + \left(\frac{\dot{m}^2}{4\pi\rho Rh}\right)_{j-out} = \dot{m} \cdot V_{j\text{-}out} + \frac{1}{2}\dot{m} V_{j-out} \tag{8}$$

Therefore, due to the presence of the Coandă blanket, the Coandă MAV has additional lift given in (8). It should be noted that a more exact approach requires additional information, i.e. the energy conservation equation, which is then utilized as the fourth equation. This is elaborated subsequently.

Applying the energy conservation equation on the same control volume, which has been redrawn for convenience in Figure 4, assuming uniform properties across the sectional areas at the input and output of the Coandă jet blanket. Ignoring the entrainment energy exchange between the ambient air and the Coandă jet blanket, the energy equation can be written as:

$$\left(\frac{p}{\rho}\right)_{in} + \frac{1}{2}\left(V_{j\text{-}in}^{\ 2}\right) = \left(\frac{p}{\rho}\right)_{out} + \frac{1}{2}\left(V_{j\text{-}out}^{\ 2}\right) \tag{9}$$

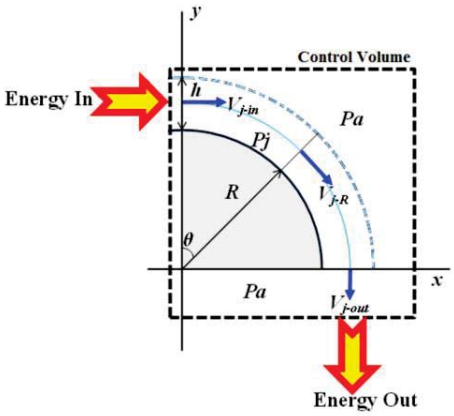

Figure 4: Schematic of the control volume around the MAV for the application of the energy conservation equation

which is essentially the Bernoulli equation along any streamline between the inlet and the outlet sections. The contribution of the entrainment energy exchange along the Coandă jet blanket can later be incorporated, such as by adopting certain assumptions as a heuristic approach or, applying the complete viscous equation by numerical simulation or CFD approach. The latter should be carried out for more meticulous approach, using the present simplified analytical approach as guidelines. At the same time, the CFD results, by appropriate considerations of the relevant parameters utilized there can be used in

developing the heuristic approach as well as for validating and assessing the merit of the analytical approach. Noting that from the outset, the flow is considered to be incompressible, equation (9) reduces to:

$$\frac{1}{2}\rho V_{\text{j-in}}^{2} = \frac{1}{2}\rho V_{\text{j-out}}^{2} \tag{10}$$

Hence, by the application of the conservation energy principle for incompressible flow, and assuming ambient pressure at the inlet and outlet of the Coandă jet blanket and neglecting the energy exchange between the ambient air and the Coandă jet blanket, the following velocity relationship between the inlet and outlet sections of the Coandă jet blanket is given by

$$V_{j\text{-}out} = V_{j\text{-}in} \tag{11}$$

This latter equation can eliminate the use of the earlier assumption taken to relate the inlet and outlet velocity by a plausible heuristic assumption (which can be established by using CFD results), and replace it by equation (11). This should simplify the solution given in equation (8) and reduce the use of idealization or the number of assumption since fewer unknowns are included in the equations. Combining equations (8) and (11)

$$Lift_{\substack{Coanda-jet\ Blanket+ \\ induced\ pressure\ difference}} = \frac{3}{2}\dot{m}V_{j-in} \tag{12}$$

The results will be assessed a posteriori by using more structured CFD simulations, although the latter may also contain uncertainties and inaccuracies.

3. Flight Dynamic Analysis for Semi-spherical Coandă MAV in Translatory Motion

3.1. System of Coordinates

For the derivation of the equation of motion of the Coandă MAV, the system coordinates that are required for setting the equation will be defined. Following the convention in flight dynamics, four main reference frames are identified, namely the inertial coordinate system, the local horizon reference frame, the body reference frame, and the wind reference frame, as required in the analysis, and are depicted in Figure 5a.

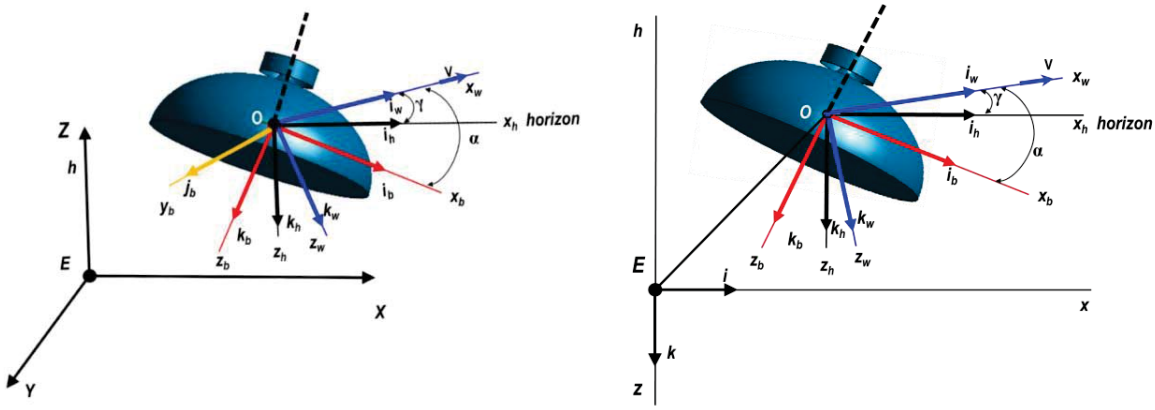

Figure 5: (a) The details of the four coordinate systems for Coandă MAV flight vehicle; (b) Axes systems in the vertical plane perpendicular to the Earth's Surface

Without loss of generality, for simplicity and instructiveness, only two-dimensional coordinate systems in the plane of symmetry of the Coandă MAV will be elaborated. These four coordinates are:

1. ***Inertial coordinate system***, which is used for defining and the application of the Newton's law of motion. In two dimensions, this coordinate system is depicted by the $O_E xyz$.

2. ***The local horizon coordinate system*** $Ox_hy_hz_h$, which is fixed at the center of mass of the vehicle, and is parallel with the earth Inertial Coordinate system.
3. ***The body coordinate system*** $Ox_by_bz_b$, which is fixed to the vehicle and follows a conveniently chosen axis of the vehicle.
4. ***The wind axes system*** $Ox_wy_wz_w$, which moves with the vehicle and the x_w axis is coincident with the velocity vector (flight path of the vehicle).

In the figure, the wind axes are oriented to the flight path angle γ relative the local horizon axes and by the angle of attack α relative to the body axes. The two dimensional configuration in the vertical plane perpendicular to the earth surface is shown in Figure 5b.

3.2. Flight Dynamic Analysis

In the development of the flight dynamics of Coandă MAV in translatory motion, without loss of generalities, the equation of motion is developed in the vertical plane perpendicular to the earth motion, rendering two-dimensional planar motion. The hovering state, as depicted in Figure 6, will be utilized as a reference.

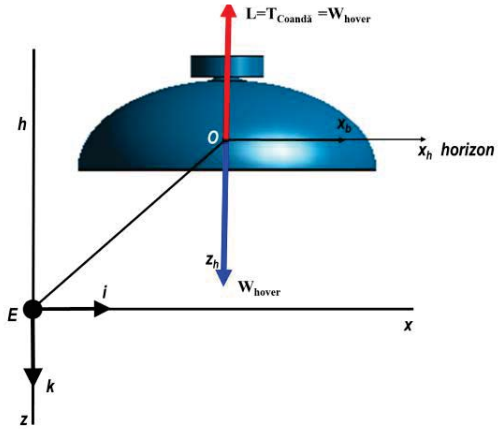

Figure 6: Coordinate systems for Coandă MAV in hover, in two-dimensional configuration (at the vertical plane of symmetry and motion)

Balance of forces in the free-body diagram exhibited in Figure 6 and the use of the Coandă lift from equation (12) leads to:

$$L_{Hover} \equiv T_{Coandă-MAV} = \frac{3}{2}\dot{m} \cdot V_{j\text{-}in} = 3\pi\rho R_i h_i V_{j\text{-}in}^2 = W_{Coandă-MAV-Take-off} \tag{13}$$

In the development of the equation of motion during translatory motion, a further simplifying assumptions will be made, which could be refined at later stage to incorporate more realistic ones.
These are:

1. The thrust of the Coandă MAV will not be affected by the attitude of the Coandă MAV configuration during hover. Such simplifying assumption can be later modified using more elaborate analytical model, assisted by CFD simulation.
2. During the translatory motion, the thrust of the Coandă MAV is assumed to be:

$$T_{Coandă-MAV} = \frac{3}{2}\dot{m} \cdot V_{j\text{-}in}\Big|_{hover-equivalent} = 3\pi\rho R_i h_i V_{j\text{-}in}^2\Big|_{hover-equivalent} \tag{14}$$

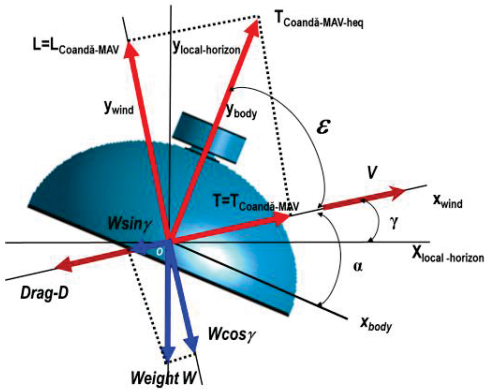

Figure 7: Schematic of Coandă MAV in two-dimensional tranlatory motion in the vertical plane (at the vertical plane of symmetry and motion).

The equation of motion of the Coandă MAV in translational motion in the two-dimensional vertical plane can be written by referring to Figure 7 using the basic flight dynamic equation for flight vehicle:
Kinematic:

$$\dot{x} = V\cos\gamma \qquad \left[LT^{-1}\right] \qquad (15)$$

$$\dot{h} \equiv \dot{y} = V\sin\gamma \qquad \left[LT^{-1}\right] \qquad (16)$$

$$\varepsilon = tan^{-1}\frac{\ddot{y}_{wind}}{\dot{V}} = tan^{-1}\frac{g\left(L - W\cos\gamma\right)}{W\dot{V}} \qquad [-] \qquad (17)$$

$$\dot{\varepsilon} = tan^{-1}\frac{\ddot{y}_{wind}}{V} = tan^{-1}\frac{g\left(L - W\cos\gamma\right)}{WV} \qquad \left[T^{-1}\right] \qquad (18)$$

Coandă MAV Fluid Dynamics:

$$T_{Coandă-MAV-heq} \equiv T_{Coandă-MAV-hover-equivalent} = \frac{3}{2}\dot{m}\cdot V_{j\text{-}in} = 3\pi\rho R_i h_i V_{j\text{-}in}^2 \qquad \left[MLT^{-2}\right] \qquad (19)$$

$$T_{Coandă-MAV-heq} \equiv T_{Coandă-MAV-hover-equivalent} = \frac{3}{2}\dot{m}\cdot V_{j\text{-}in} = \frac{3}{2}\dot{m}\cdot\frac{\dot{m}}{2\pi\rho R_i h_i} = \frac{3}{4}\frac{\dot{m}^2}{\pi\rho R_i h_i} \qquad \left[MLT^{-2}\right] \qquad (20)$$

Coandă MAV Flight Dynamics:

$$\dot{V} = \left(g/W\right)\left(T_{Coandă\ MAV-heq}\cos\varepsilon - D - W\sin\gamma\right) \qquad \left[LT^{-2}\right] \qquad (21)$$

$$\ddot{y} = \left(g/W\right)\left(T_{Coandă\ MAV-heq}\sin\left(\varepsilon+\gamma\right) - W - D\sin\gamma\right) \qquad \left[LT^{-2}\right] \qquad (22)$$

Weight-Fuel Consumption:

$$\dot{W} = -CT \qquad \left[MT^{-1}\right] \qquad (23)$$

It should be noted, that the above relationships are derived for balance of forces and Newton's equation for semi-spherical Coandă MAV treated as a point mass moving in a plane perpendicular to the planar Earth.

4. Performance Measure

4.1. Performance Measure during hover

The feasibility of using Coandă techniques to enhance aerodynamic performance of Coandă MAV can be outlined through some non-dimensional quantities of performance measure. The most logical measure that has commonly been utilized is the Coandă jet momentum coefficient, C_μ (Mamou and Khalid [14], 2007; Djojodihardjo [9]), which are defined as:

$$C_\mu = \frac{\dot{m} V_{Coandă-jet}}{\frac{1}{2}\rho_j V_\infty^2 A_{ref}} \qquad (24)$$

While (24) may be appropriate for any Coandă activated vehicle (i.e. Coandă MAV), particularly during hover and lift-off, one can define another performance measure to evaluate the aerodynamic performance for spherical Coandă MAV considered here, by assessing the output lift as compared to the input momentum rate, following consideration discussed by Djojodihardjo and Ahmed [12], and is given by:

$$PM1_{\substack{Spherical\ Coandă- \\ MAV}} = \frac{Lift_{Coanda-jet\ Blanket+induced\ pressure\ difference}}{Coanda\ Jet\ Momentum\ In} = \frac{3}{2} \qquad (25a)$$

Alternatively, this obvious dimensionless performance measure may be defined based on the rate of the energy of the Coandă jet ejected by Coandă MAV at its ideal inlet velocity $V_{j\text{-}out}$ at its peripheral outlet compared to the rate of momentum influx of the Coandă jet times its inlet velocity $V_{j\text{-}in}$ (non-dimensional):

$$PM3_{\substack{Spherical \\ Coandă-MAV}} = \frac{Lift\ produced\ by\ Coandă\ MAV\ times\ V_{j-out}\ at\ its\ peripheral\ outlet}{the\ rate\ of\ momentum\ influx\ of\ the\ Coandă\ jet\ times\ its\ inlet\ velocity\ V_{j-in}}$$

$$= \frac{Lift.V_{j-out}}{2\pi R_0 h_0 \rho V_{j\text{-}in}{}^2 \cdot V_{j\text{-}in}} = \frac{\frac{3}{2}\dot{m} V_{j-in}{}^2}{2\pi R_0 h_0 \rho V_{j\text{-}in}{}^3} = \frac{3\pi R_0 h_0 \rho \cdot V_{j\text{-}in}{}^3}{2\pi R_0 h_0 \rho \cdot V_{j\text{-}in}{}^3} = \frac{3}{2} \qquad (25b)$$

$$= 3\rho A_{MAV\_base}\left(\frac{h_0}{R_0}\right)$$

It is realized at this point, that more information is required to insure uniqueness. Resorting to the present heuristic approach, further realistic assumption can be drawn from CFD visualization, which also added further insight to the problem. Similar expression can be defined for Cylindrically Shaped Coandă MAV.

Alternatively, it may be noted that Mirkov and Rasuo [15-16] considered the inlet velocity to thrust ratio for a given inlet size could be the most important output value resulting either from experiment on UAV's or by numerical simulation. In view of that, another performance measure could be defined to be the lift to inlet velocity, which is a dimensional quantity and substituting equation (13) for the lift, it gives;

$$PM2_{\substack{Spherical \\ Coandă-MAV}} = \frac{Lift_{Coanda-jet\ Blanket+induced\ pressure\ difference}}{Coandă\ jet\ inlet\ Velocity} = \frac{\dot{m} \cdot V_{j\text{-}in} + \frac{1}{2}\dot{m} V_{j-in}}{V_{j\text{-}in}} = \frac{3}{2}\dot{m} \qquad (26)$$

A third performance measure may be defined based on the Coandă jet rate of momentum influx per unit Coandă jet kinetic energy input (dimensional):

$$PM3_{\substack{Spherical\\Coandă-MAV}} = \frac{Lift_{Coanda-jet\,Blanket+induced\,pressure\,difference}}{Jet\ Inlet\ velocity^2} = \frac{2\pi R_0 h_0 \rho \cdot V_{j\text{-}in}{}^2 + \pi R_0 h_0 \rho V_{j-in}{}^2}{V_{j\text{-}in}{}^2}$$
$$= 3\rho A_{MAV\_base}\left(\frac{h_0}{R_0}\right) \tag{27}$$

where

$$A_{MAV\_base} = \pi R_0{}^2 \tag{28}$$

4.2. Performance Measure during translation

As a baseline, performance measure during translation can be defined for two cases:

For level flight

For climbing

For level flight (by referring to Figure 7):

$$PM_{\substack{Coandă-MAV\\LevelFlight}} = \frac{Power\ required\ to\ overcome\ Drag}{Power\ Input\ by\ Coandă\ jet\ action} = \frac{Drag * Velocity}{Coandă\ Jet\ Momentum\ Gain * Coandă\ Jet\ Velocity\ In}$$
$$= \frac{D \cdot V\cos\gamma^2}{\dot{m}V_{j\text{-}in}{}^2} \qquad \left[\frac{ML^2T^{-2}}{ML^2T^{-2}}\right] \tag{29}$$

For purely level flight, as depicted in Figure 8, γ=0, and Equation (29) reduces to:

$$PM_{\substack{Coandă-MAV\\LevelFlight}} \approx \frac{1}{4}C_{D\to x}\frac{\pi\rho R_o{}^2\sin\alpha}{\dot{m}_i}\frac{V^3}{V_{j\text{-}in}{}^2} \tag{30}$$

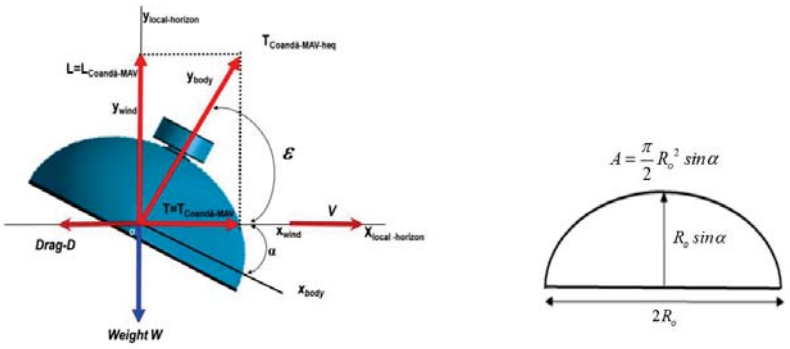

Figure 8: Schematic of Coandă MAV in two-dimensional cruising motion in the vertical plane of symmetry and motion. Inset: Cross sectional area perpendicular to direction of motion.

For climbing:

$$PM_{\substack{Coandă\\-MAV\\Climbing}} = \frac{Power\ required\ to\ Climb}{Power\ Input\ by\ Coandă\ jet\ action} = \frac{\mathbf{T}_{Coandă-MAV-heq}\bullet\dot{\mathbf{y}} - \mathbf{D}\bullet\dot{\mathbf{y}} - \mathbf{W}\bullet\dot{\mathbf{y}}}{Coandă\ Jet\ \text{Momentum Gain} * Coandă\ Jet\ \text{Velocity In}}$$
$$= \frac{3}{2}\frac{\cos(\alpha-\gamma)V\sin\gamma}{V_{j\text{-}in}} - \frac{(D\sin\gamma + W)V\sin\gamma}{\dot{m}V_{j\text{-}in}{}^2} \qquad \left[\frac{ML^2T^{-2}}{ML^2T^{-2}}\right] \tag{31}$$

For purely climbing flight, γ=π/2, and Equation (29) reduces to

$$PM_{\substack{\text{Coandă-MAV}\\ \text{Climbing}}} = \frac{\frac{3}{2}\dot{m}\cdot V_{j\text{-}in}V - \left(\frac{1}{2}\rho C_{D\to y}\pi R_o^{\,2}V^2 + W\right)V}{\dot{m}V_{j\text{-}in}^{\,2}} = \frac{\frac{3}{2}\dot{m}\cdot V_{j\text{-}in}V - \left(\frac{1}{2}\rho C_{D\to y}\pi R_o^{\,2}V^2 + \left(\frac{3}{2}\dot{m}V_{j-in}\right)_{hover}\right)V}{\dot{m}V_{j\text{-}in}^{\,2}} \quad (32)$$

Which has been further developed from that given in [16]. The Performance Measure $PM_{\text{Coandă-MAV Level Flight}}$ can be expressed as a function of C_D, R_o, $\dot{m}$, h_i, α, V, $V_{j\text{-}in}$. These are the basic relationships that can further be modified and elaborated for other flight conditions.

5. Some Results and Examples

5.1. Results and examples for hover

To assess the merit and plausibility of the theoretical analysis using first principles carried out here, a comparison of the theoretical prediction for the performance measures PM1, PM2 and PM3 given by (25) - (27) are compared with CFD simulation carried out using ANSYS FLUENT® for Spherically Shaped Coandă MAV. The results are depicted in Figures 9 and 10.

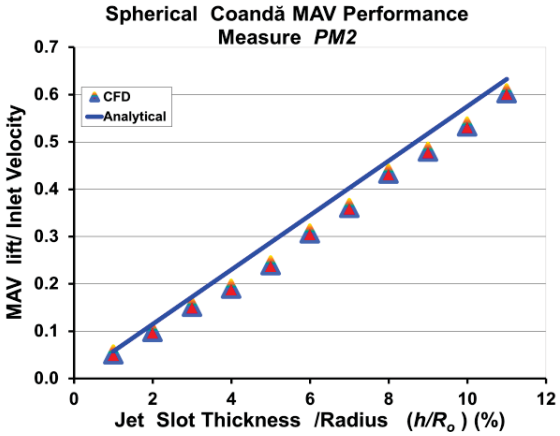

Figure 9: Performance measure for spherical Coandă MAV for various Jet slot thickness at different jet velocity.

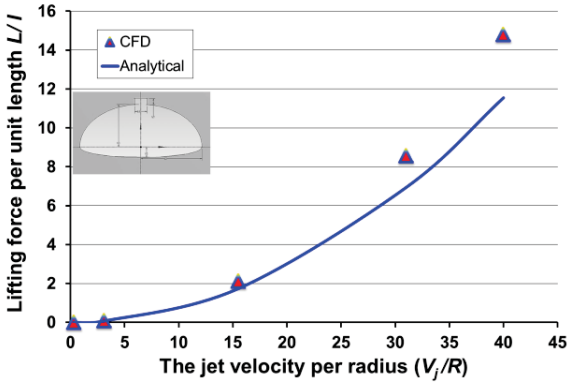

Figure 10: Analytical and CFD models comparison for jet inlet velocity influence on performance of Spherical Coandă MAV at constant jet thickness (h=50mm).

The CFD simulation was performed using steady RANS with two equations k-ω Shear Stress Transport (SST) turbulence model. Simple pressure-velocity coupling scheme with the least squares cell base as discretization gradient was applied in the solution method together with second order upwind for the momentum equation and the turbulent kinetic energy.

As depicted in Figure 9, the influence of the ratio of the jet slot thickness h to the reference radius R_o which influence the jet inlet velocity on the performance measure PM2 is clearly noticeable. In addition to the above performance measures, the influence of the jet inlet velocity on the Coandă MAV lift may also be of interest from designer's point of view which enables them to befittingly select the right propulsion system for such MAV. The jet inlet velocity influence on performance of Spherical Coandă MAV at constant jet thickness (h=50mm) is depicted in Figure 10.

For Cylindrical Coandă MAV the corresponding theoretical prediction for PM2 is given by [11-12]

$$PM2_{\substack{Cylinderical\\ Coandă-MAV}} = \frac{Lift_{Coanda-\,jet\,Blanket+induced\,\,pressure\,difference}}{Coandă\,\,jet\,inlet\,Velocity} = \frac{\rho V_{j-in}^2 l\left(\frac{h^2}{t}\right)+\frac{1}{2}\rho\left(\frac{h}{t}V_{j-in}\right)^2 Rl}{V_{j\text{-}in}} \tag{33}$$

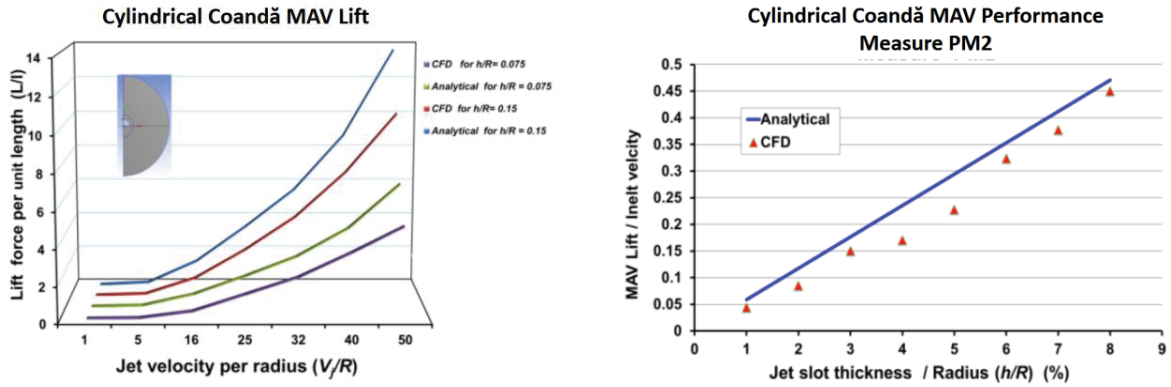

Figure 11: Performance measure comparison between mathematical and CFD models for Cylindrical Coandă MAV for various (a) Inlet velocity and (b) Jet slot thickness

For comparative and validation purposes, Figure 11 (a) and (b) are produced and compared to CFD simulation results to assess the present theoretical prediction with CFD simulation results a cylindrical Coandă MAV. Relatively good qualitative agreements between the theoretical results and CFD simulations shown there lend support to the present analysis, noting that in the analytical study carried out here many simplification have been introduced, while in the CFD simulation, the full Navier-Stokes equation for incompressible fluid was used.

The effect of viscosity that can be revealed by CFD simulation is exemplified by Figure 12 for two different locations of the Coandă jet introduction. The CFD images exhibited in Figure 12 (a) and (b) show the velocity magnitude contours for the given configuration and inlet conditions for cases considered by Mirkov and Rasuo [17-18] and Ghozali [19].

Figure 13 shows structured numerical mesh used in the flow domain. Through meticulous attempts and grid sensitivity studies the size of the mesh cells was generated small to enable visualizations of the flow around the whole body with best details. The numerical study was performed with a moderately small Reynolds number, Re= 68458, based on mean velocity and jet inlet height. The velocity is uniform ($V_{j\text{-}in}$ = 20 m/s) across the inlet which has a thickness of 0.05 m. The number of the mesh cells was 52830, and the

mesh quality was found to be acceptable. The orthogonality quality was 4.96943e-01, which should be acceptable from the ANSYS orthogonality quality requirements. As elaborated by Ahmed and Djojodihardjo [10-11] and Djojodihardjo and Ahmed [12-13], the present generation of mesh is considered to be acceptable.

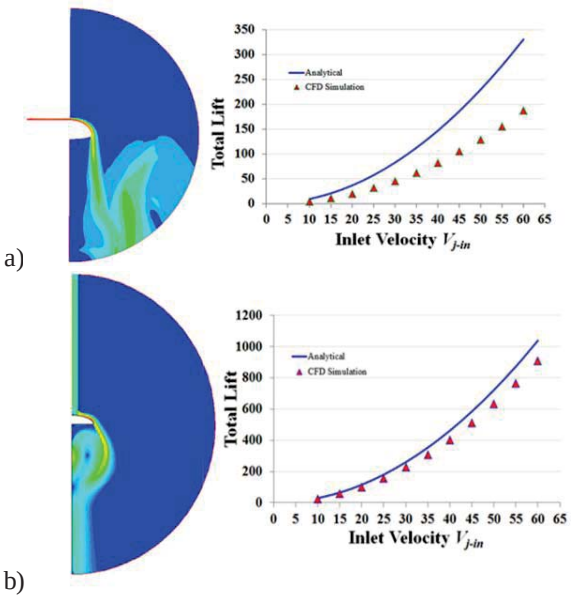

Figure 12: Lift versus input jet velocity for similar configuration considered in (a) Mirkov and Rasuo [17], (b) Ghozali [19]

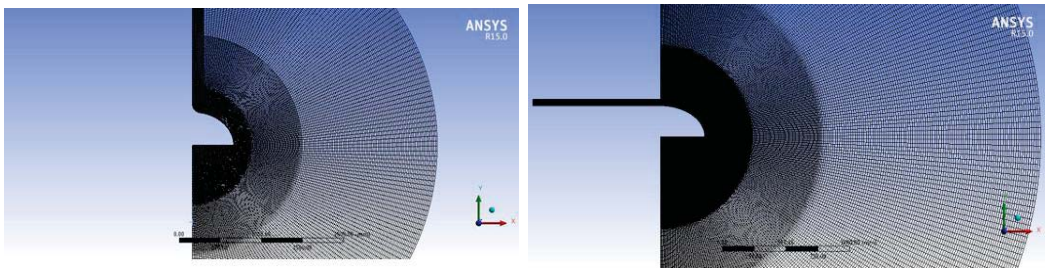

Figure 13: Mesh details for similar configuration considered in (a) Mirkov and Rasuo [18], (b) Ghozali [19]

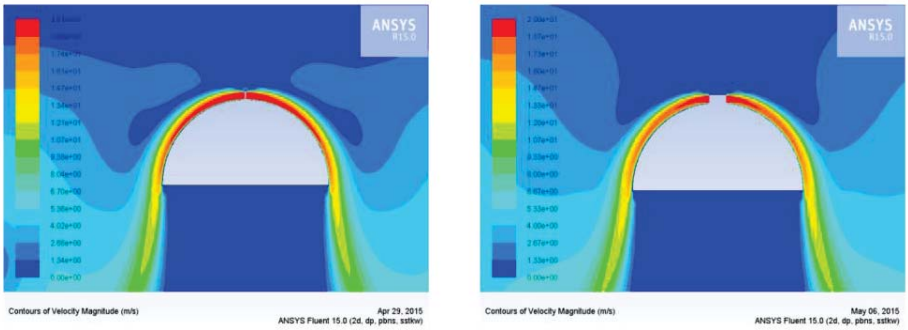

Figure 14: Symmetrical Coandă effect - velocity magnitude contour with different inlet radius a) R_i=5 mm, b) R_i=50mm

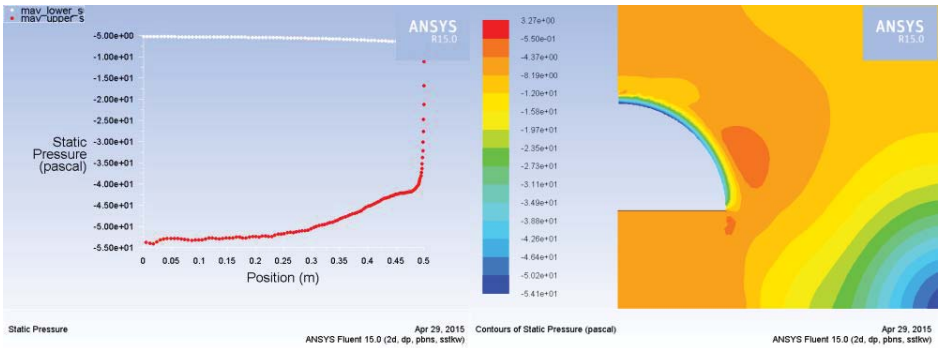

Figure 15: Comparison between the CFD simulation and plot for pressure contours along semi-spherical Coandă MAV surface.

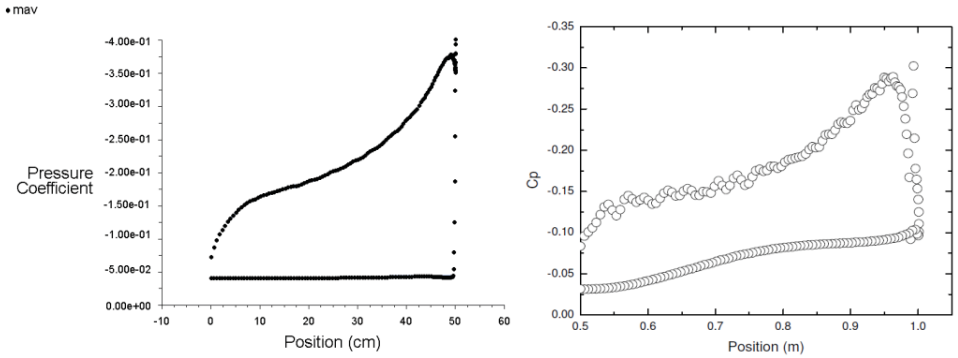

Figure 16: Comparison of the coefficient of pressure on the Coandă MAV surface jet blanket; a. present CFD Simulation, b. simulation by Mirkov and Rasuo [18].

The influence of the inlet jet radius on the air vehicle performance (lift) is also investigated using the CFD simulation, The results are presented as velocity magnitude contours, which were carried out for two inlet jet radius, R_i=5 mm and R_i=50mm and as shown in Figure 14. For the semi-spherical Coandă MAV, the CFD simulation and visualization results are exhibited in Figure 15, which exhibit the pressure contours along semi-spherical Coandă MAV surface obtained by CFD simulation results (left), and the associated static pressure color-coded contour (right).

The CFD numerical study presented here was performed with a moderately small Reynolds number, Re= 68458, based on mean velocity and jet inlet height. The velocity across the inlet, which has a thickness of 0.05 m, is uniform (*Vj-in* = 20 m/s). The number of the mesh cells was 52830, and the mesh quality was found to be acceptable. The orthogonality quality was 4.96943e-01, which is acceptable from the ANSYS orthogonality quality requirements.

5.2. Results and examples for translation

For translatory flight, some examples of Performance Measures simulation studies for Coandă MAV in purely level and climbing flights are exhibited by Figs. 17 and 18, obtained using equations (30) and (32) for level and climbing flights, respectively. Fig. 17 shows the influence of Coandă jet slot thickness on the cruise performance for various Coandă jet inlet velocity, while Figure 18 shows pure Coandă MAV climbing performance for various Coandă jet slot thickness and inlet velocity. The latter figure shows the threshold of these parameters that will provide Coandă MAV climbing capability.

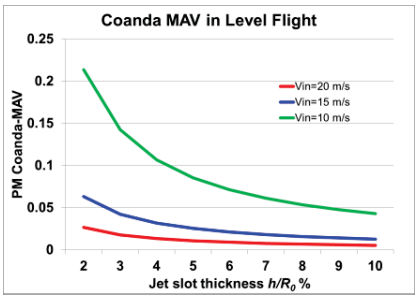

Figure17: Coandă MAV Performance Measure as a function of jet slot thickness for various cruising velocity, calculated using Eq. (29) and CFD simulation for a baseline Coandă MAV configuration.

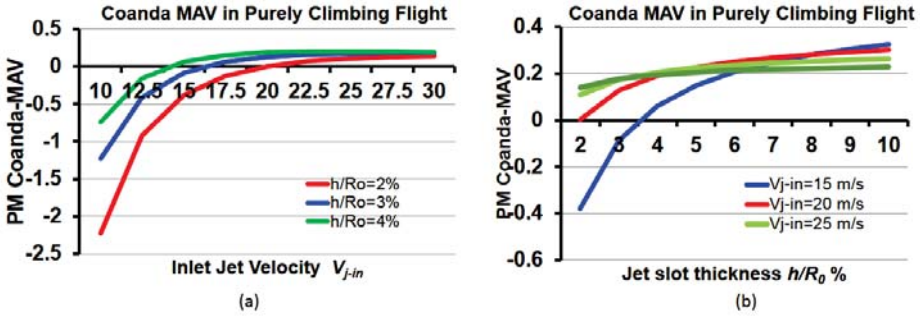

Figure 18: Coandă MAV Performance Measure as a function of jet slot thickness for various climbing rate (velocity), calculated using Eq. (31) and CFD simulation for a baseline Coandă MAV configuration; (a) Climbing Performance as function of Coandă jet velocity at various jet slot thickness, (b) Climbing Performance as function of Coandă jet slot thickness at various jet velocity.

Parametric study results exhibited by these figures can be utilized to give insight on the performance of the semi-spherical Coandă MAV considered as well as for preliminary sizing purposes.

6. Conclusions

A comprehensive effort has been made to analyze and describe the governing equations applicable to Coandă MAV in hover and translatory motion utilizing first principles as articulated in fluid dynamics, using conservation principles for control volume analysis, and flight mechanics, using free-body diagram analysis for the application of Newton's law of motion. The basic working relationships among various relevant variables and parameters governing the aerodynamics forces and performance measures of Coandă MAV in hover and translatory motion are then established.

CFD simulations for the Coandă MAV generic models considered are carried out with two objectives, to gain insight into the flow situation for establishing the analytical model, and to assess and validate the analytical model subject to the theoretical assumptions.

Various CFD studies have also indicated that there are still significant discrepancies between CFD and experimental studies [6], which necessitate the existence of specific baseline configurations for validation purposes.

From the theoretical analysis, performance measures are derived as further elaboration of the significance of Coandă jet momentum coefficient, which are shown to be capable in assessing the effectiveness of the Coandă jet as lift generating mechanism of the and Coandă MAV, as well as its propulsion mechanism in the Coandă MAV flight.

Comparison of the theoretical analysis using first principles on the Coandă MAV generic configurations with Reynolds averaged Navier Stokes CFD simulation using appropriate turbulence model serves also to assess the uncertainties and accuracy of the theoretical approach. In addition, the CFD computational and visualization studies, can provide further insight in revealing other characteristics of the flow field, and can assist further in-depth analysis, as well as in the design of experiments to that end. For example, to find out the effect of viscosity, Coandă jet input variables and Coandă MAV jet blanket on the Coandă jet stability and attachment. CFD visualization has certainly assist the analytical work in assessing the application of fundamental conservation principle in continuum mechanics as well as elaborating the equation of motion for the flight dynamics of the Coandă MAV.

References

[1] Gad-el-Hak M 2000 Flow Control - Passive, Active and Reactive Flow Management (Cambridge University Press, London)
[2] Liu Y, Sankar L N, Englar R J, Ahuja K K 2001 Numerical Simulations of the Steady and Unsteady Aerodynamic Characteristics of a Circulation Control Wing Airfoil *AIAA Paper* **2001-0704**
[3] Kweder J, Panther C, Smith J E 2011 Applications of circulation control, yesterday and today *International Journal of Engineering, (IJE)* **195 vol.4 (5)**, pp. 411-429
[4] Djojodihardjo H and Thangarajah N 2014 Research, development and recent patents on aerodynamic surface circulation control-A critical review *Recent Patents on Mechanical Engineering* **vol. 7**, pp. 1-37.
[5] Djojodihardjo H 2013 Progress and development of Coandă jet and vortex cell for aerodynamic surface circulation control – An overview *The SIJ Transactions on Advances in Space Research & Earth Exploration (ASREE)*, **Vol. 1, No. 1**, September-October.
[6] Rumsey C L and Nishino T 2011 Numerical study comparing RANS and LES approaches on a circulation control airfoil International Journal of Heat and Fluid Flow **32** 847-864.
[7] Tongchitpakdee C, Benjanirat S and Sankar L N 2006 Numerical Studies of the Effects of Active and Passive Circulation Enhancement Concepts on Wind Turbine Performance *J.Sol.Energy Eng* **128(4)** 31023089
[8] Abdul-Hamid, M F, Djojodihardjo H, Suzuki S and Mustapha F 2010 Numerical Assessment of Coanda Effect as Airfoil Lift Enhancer in Wind-Turbine Configuration, *Regional Conference on Mechanical and Aerospace Technology* Bali, February 9 – 10
[9] Djojodihardjo H, Abdul-Hamid M F, Jaafar A, Basri S, Romli F I, Mustapha F, Mohd-Rafie A S and Abdul-Majid D L A 2013 Computational Study on the Aerodynamic Performance of Wind Turbine Airfoil Fitted with Coandă Jet *Journal of Renewable Energy* **2013**, 839319
[10] Djojodihardjo H, Ahmed R I 2016 CFD Simulation of Coandă Effect on the Upper Respiratory System *Journal of Medical Imaging and Health Informatic* in print
[11] Ahmed R I, Djojodihardjo H, Abu-Talib A R, Abd-Hamid M F 2014 Application of Coandă jet for generating lift for micro air vehicles – Preliminary design considerations, *Applied Mechanics and Materials* **629** 139-144
[12] Ahmed R I, Djojodihardjo H, Abu-Talib AR, Mohd-Rafie A S 2016 First Principle Analysis of Coandă Micro Air Vehicle Aerodynamic Forces for Preliminary Sizing *Aircraft Engineering and Aerospace Technology* DOI: 10.1108/AEAT-03-2015-0080.R2 in print,
[13] Djojodihardjo H and Ahmed R I 2014 An Analysis on the Lift Generation for Coandă Micro Air Vehicles *IEEE, ICARES conference proceeding*, Yogyakarta.
[14] Djojodihardjo H, Ahmed R I, Abu-Thalib A R and Mohd-Rafie A S 2015 Analytical and CFD visualization studies of Coandă MAV *Proceedings The 13th Asian Symposium on Visualization* Novosibirsk
[15] Mamou M and Khalid M 2007 Steady and unsteady flow simulation of a combined jet flap and Coanda jet effects on a 2D airfoil aerodynamic performance *Revue des Energies Renouvelables* **CER'07 Oujda** 55 – 60
[16] Djojodihardjo H and Ahmed R I 2016 Analytical, Computational Fluid Dynamics and Flight Dynamics of Coandă MAV, *conference paper ICAS2016_0114, 30th International Congress of the International Council of the Aeronautical Sciences*, Daejon.
[17] Mirkov N and Rasuo B 2019 Numerical Simulation of Air Jet Attachment to Convex Walls and Applications *ICAS 2010-621*
[18] Mirkov N and Rasuo B 2012 Maneuverability of a UAV with Coanda Effect Based Lift Production *ICAS 2012-617*
[19] Ghozali D 2013 Analysis of Coandă Effect Using Computational-Fluid-Dynamic, *Thesis, Universitas Gajah Mada,* Indonesia

Acknowledgement

The authors would like to thank Universiti Putra Malaysia (UPM) for granting Research University Grant Scheme (RUGS) No.9378200, and the ministry of higher education ERGS: 5527088 ; FRGS:5524250 under which parts of the present research is carried out.